


 Cite this: *Chem. Commun.*, 2019, 55, 2372

 Received 23rd January 2019,  
 Accepted 28th January 2019

DOI: 10.1039/c9cc00599d

rsc.li/chemcomm

## Tetraphenylethene-based tetracationic cyclophanes and their selective recognition for amino acids and adenosine derivatives in water†

 Lin Cheng,<sup>‡a</sup> Haiyang Zhang,<sup>‡a</sup> Yunhong Dong,<sup>‡ab</sup> Yanxia Zhao,<sup>a</sup> Yang Yu<sup>a</sup> and Liping Cao  <sup>\*a</sup>

**Two new tetracationic cyclophanes 1 and 2 containing tetraphenylethene and bipyridinium moieties were synthesized via a two-step S<sub>N</sub>2 reaction. These water-soluble cyclophanes with a cationic and hydrophobic cavity exhibited selective recognition for amino acids (e.g. tryptophan) and adenosine derivatives (e.g. ATP) via electrostatic and π–π interactions in water.**

Synthesis, recognition and self-assembly of supramolecular hosts (e.g. clips, macrocycles, cages, and capsules) have played important roles in the development of supramolecular chemistry.<sup>1</sup> Several famous macrocyclic compounds, such as crown ether,<sup>2</sup> cyclodextrin,<sup>3</sup> calixarene,<sup>4</sup> cucurbituril,<sup>5</sup> cyclophane,<sup>6</sup> and pillararene,<sup>7</sup> have already attracted attention from the chemical community to explore the nature of molecular interactions and construct supramolecular architectures/machines. Particularly, cationic cyclophanes with various sizes, shapes, and functional groups have been widely used, because of not only their unique electron-deficient cavity for selectively binding guest molecules, but also their reduction–oxidation properties for electronic devices<sup>8</sup> (e.g. semiconductor) and molecular machines<sup>9</sup> (e.g. molecular shuttle and molecular pump). The most famous one is Stoddart's 'Blue Box', as a classic cationic cyclophane, which has milestone significance for the synthesis and development of new cationic cyclophanes.<sup>10</sup> The cationic cyclophane and its derivatives can form stable complexes with a series of electron-rich guest molecules through non-covalent bonds for the construction of many complicated supramolecular structures, such as catenanes,<sup>11</sup> rotaxanes,<sup>12</sup> nano-conductive

materials,<sup>13</sup> electrochemically switchable molecules,<sup>14</sup> metal-organic frameworks (MOFs),<sup>15</sup> and so on.

Tetraphenylethene (TPE) as a typical aggregation-induced emission (AIE) luminogen has been widely applied to fabricate and construct fluorescent systems with carbohydrates, lipids, amino acids, proteins, enzymes, nucleic acids, and others.<sup>16</sup> In supramolecular chemistry, TPE derivatives have also been used as building blocks for the design and synthesis of macrocyclic compounds or assemblies.<sup>17–19</sup> For example, Zheng and co-workers reported a series of TPE-based macrocycles and cages with an AIE effect for functional applications, such as chiral recognition,<sup>17a</sup> self-assembly,<sup>17b</sup> and gas sorption.<sup>17c</sup> Stang and co-workers developed a series of pyridyl TPE-based platinum(II) metallacycles<sup>18</sup> and metallacages,<sup>19</sup> which exhibited high emission based on their AIE properties in various solvents. Although several cationic cyclophane derivatives have been effectively utilized for host–guest complexation, the synthesis and host–guest study of water-soluble cyclophanes that retain the recognition ability in aqueous media still remain a huge challenge.<sup>20</sup> Here we report the synthesis and characterization of two cationic cyclophanes (**1** and **2**) containing tetraphenylethene (TPE) and bipyridinium (BP) moieties, which have a suitable cavity for selectively recognizing amino acids (e.g. tryptophan) and adenosine derivatives (e.g. ATP) in water.

Cationic cyclophanes (**1** and **2**) were synthesized *via* two-step S<sub>N</sub>2 reactions as shown in Scheme 1 (see the ESI†): (1) the first-step S<sub>N</sub>2 reaction between **3** and dipyrindine gives a C-shaped compound (**4**) in 97% yield; (2) the second-step S<sub>N</sub>2 reaction between **4** and the corresponding dibromide compounds (**3** or **5**) proceeds through a cyclic formation to give **1** and **2** with PF<sub>6</sub><sup>−</sup> as counterions in 35% and 42% yields without chromatography, respectively. Finally, **1** and **2** were transformed to their Cl<sup>−</sup> form upon adding an excess amount of tetrabutylammonium chloride in 90% and 85% yield, respectively. **1** and **2** with Cl<sup>−</sup> as counterions showed a good solubility of ~49.0 mM and ~3.4 mM in D<sub>2</sub>O as determined by NMR, indicating their potential application for molecular recognition in water (Fig. S15 and S16, ESI†).

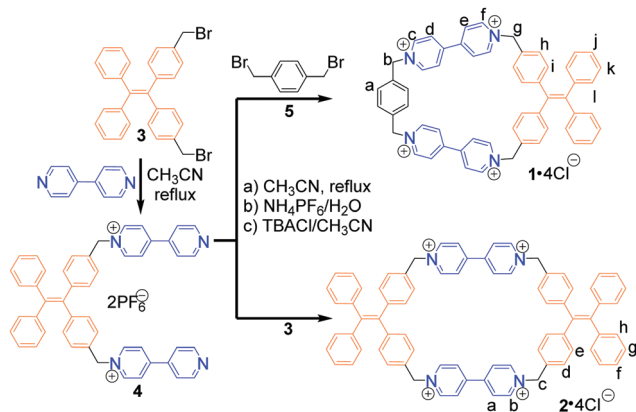
The cyclic structure and cavity size of cyclophanes **1** and **2** were further confirmed by single crystal X-ray analysis (Fig. 1).

<sup>a</sup> Key Laboratory of Synthetic and Natural Functional Molecule Chemistry of the Ministry of Education, Northwest University, Xi'an, 710069, P. R. China.  
 E-mail: chcaoliping@nwu.edu.cn

<sup>b</sup> National Demonstration Center for Experimental Chemistry Education, College of Chemistry and Materials Science, Northwest University, Xi'an, 710069, P. R. China

† Electronic supplementary information (ESI) available: Experimental details, including synthesis, ITC, NMR, UV/vis, fluorescence, and crystal data in CIF format. CCDC 1870620 and 1870621. For ESI and crystallographic data in CIF or other electronic format see DOI: 10.1039/c9cc00599d

‡ These authors contributed equally.



Scheme 1 Synthesis of the cationic cyclophane derivatives **1** and **2**.

The X-ray quality single crystals of cyclophane **1**·4PF<sub>6</sub><sup>−</sup> were obtained by slow vapour diffusion of dichloromethane into an acetone solution of **1**·4PF<sub>6</sub><sup>−</sup> at room temperature. Cationic cyclophane **1** was found to crystallise in a monoclinic crystal system. The dihedral angle between two pyridinium rings is about 44.4° in the bipyridinium moieties. Interestingly, **1** possesses a trapezoid-like cavity with top, bottom, and side lengths of about 5.8 Å, 9.6 Å, and 9.9 Å, respectively (Fig. 1a and Fig. S17, ESI†). Furthermore, **1** exhibits a head-to-head and tail-to-tail stacking pattern to form a supramolecular framework structure (Fig. S17, ESI†). On the other hand, X-ray quality single crystals of **2**·4PF<sub>6</sub><sup>−</sup> were also obtained by slow vapour diffusion of diethyl ether into a solution of **2**·4PF<sub>6</sub><sup>−</sup> in acetonitrile/acetone at room temperature. Cationic cyclophane **2** was crystallized in a orthorhombic crystal system. Because the middle part of bipyridinium units bent into the inside of the cavity, **2** possesses a flat rectangle-like cavity with a length of about 9.9 Å and widths of ~9.8 Å at two sides and ~9.0 Å at the center (Fig. 1b). Beyond the intriguing macrocyclic cavity described above, a 3D nanotubular framework stacked by **2** molecules is revealed, which features 1D intrinsic nanotubes constructed by the cavities of **2** along the *b* axis (Fig. 1c and d). Firstly, **2** molecules are aligned parallelly to form a 1D intrinsic nanotube, in which each **2** molecule

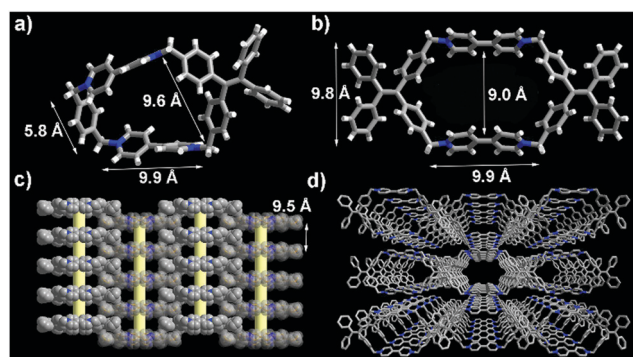
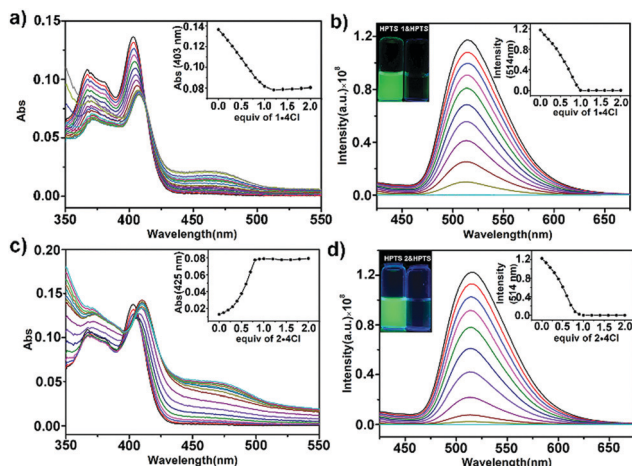


Fig. 1 The single-crystal X-ray structures of (a) a single molecule of **1**·4PF<sub>6</sub><sup>−</sup>; (b) a single molecule, (c) side view of the 2D nanotubular layer from the *c* axis, and (d) perspective view of the 3D framework of **2**·4PF<sub>6</sub><sup>−</sup> from the *b* axis, respectively. Colour code: C, grey; N, blue; H, white; and O, red. Counter ions and solvent molecules have been omitted for clarity; the atom-to-atom distances are shown here.

is closed to one another to extend through a lattice translation (~9.5 Å repeat) along the *b* axis. Secondly, the neighboring 1D nanotubes formed from **2** with a parallel arrangement form a 2D nanotubular layer in an alternate pattern (Fig. 1c). A close inspection of this 2D nanotubular layer reveals that the neighboring **2** molecules from two 1D nanotubes come into contact with each other through C–H···π interactions (Fig. S18, ESI†). Finally, the neighboring 2D nanotubular layers are stacked parallelly to form a 3D nanotubular framework (Fig. 1d). At the same time, solvent molecules (e.g. MeCN, acetone, CH<sub>2</sub>Cl<sub>2</sub>, CHCl<sub>3</sub> and Et<sub>2</sub>O) and PF<sub>6</sub><sup>−</sup> counter ions exist in the interspace of the framework structure.<sup>21</sup>

To explore the recognition ability of these cationic cyclophanes as hosts, <sup>1</sup>H NMR experiments between cyclophanes (**1** and **2**) and 8-hydroxy-1,3,6-pyrene trisulfonate (HPTS) were first performed in D<sub>2</sub>O or DMSO-*d*<sub>6</sub>. The host–guest recognition between **1** and **2** and HPTS was observed more clearly in DMSO-*d*<sub>6</sub> than in D<sub>2</sub>O, because strong electrostatic interactions between the sulfonate groups and the pyridinium ring make the host–guest complex poorly soluble in water (Fig. S19–S23, ESI†). As a result, NMR titration of **1** and **2** and HPTS confirmed the formation of 1:1 host–guest complexes in DMSO-*d*<sub>6</sub>. For example, when HPTS was added to the solution of **2**, upfield shifts of the pyrene resonances for HPTS were observed, indicating that the pyrene unit of HPTS is totally encapsulated by the cavity of **2**. Simultaneously, all resonances (H<sub>a–e</sub>) of **2** located around HPTS in the host–guest complex exhibited upfield shifts, because of the shielding effect of π-electron-rich HPTS. In addition, the COSY and NOESY spectra showed a H<sub>2</sub>–H<sub>6</sub> inter-correlation between the guest and host, indicating the formation of the inclusion complex between **2** and HPTS in DMSO-*d*<sub>6</sub> (Fig. S24, ESI†). In addition, electrospray ionization mass spectrometry (ESI-MS) confirmed the formation of the 1:1 host–guest complex between **1** and **2** and HPTS, respectively (Fig. S25 and S26, ESI†).

Subsequently, the photophysical properties of HPTS and **1** and **2** were analysed in water by fluorescence and UV-vis experiments. Like Ramaiah's anthracene-based cyclophane, **1** and **2** are non-emissive in water due to the photoinduced electron transfer (PET) from TPE to bipyridinium units.<sup>22</sup> As shown in Fig. 2a, when **1** was successively added to HPTS in water, the absorbance maximum at 403 nm decreased and moved to 408 nm, indicating the formation of the host–guest complex. And there was a new peak at 430–510 nm which may be caused by the charge-transfer interaction between HPTS and the bipyridinium units. As a result, a dramatic fluorescence quenching of HPTS at 514 nm occurred when 1.0 equiv. of **1** was added, which could be attributed to the PET from HPTS to **1** based on the formation of the host–guest complex (Fig. 2b). In addition, UV-vis and fluorescence titration experiments between **1** and HPTS gave a 1:1 stoichiometry for the complex **1**·HPTS. Similarly, UV-vis and fluorescence titration experiments of HPTS with **2** also established a 1:1 stoichiometry for the host–guest complex **2**·HPTS (Fig. 2c and d). The Job's plot obtained using UV-vis spectroscopy displayed a maximum at about 0.5, which supports a 1:1 binding stoichiometry for both complexes (Fig. S28, ESI†). Furthermore, isothermal titration calorimetry (ITC) data also confirmed that the 1:1 binding stoichiometry and the strong binding ( $K_{1,\text{HPTS}} = 4.88 \times 10^8 \text{ M}^{-1}$  and  $K_{2,\text{HPTS}} = 1.42 \times 10^9 \text{ M}^{-1}$ ) facilitate these stable host–guest complexes in water (Fig. S29, ESI†).



**Fig. 2** (a) UV-vis and (b) fluorescence titration ( $\lambda_{\text{ex}} = 365$  nm) of HPTS (5  $\mu\text{mol}$ ) with gradual addition of **1**·4Cl<sup>-</sup> in water at 298 K. The insets show a plot of absorbance intensity at 403 nm and emission intensity at 514 nm versus the equivalent of **1**·4Cl<sup>-</sup>. (c) UV-vis and (d) fluorescence titration ( $\lambda_{\text{ex}} = 365$  nm) of HPTS (5  $\mu\text{mol}$ ) with gradual addition of **2**·4Cl<sup>-</sup> in water at 298 K. The insets show a plot of absorbance intensity at 403 nm and emission intensity at 514 nm versus the equivalents of **2**·4Cl<sup>-</sup>.

Because of the appropriate size of the cavity, **2** exhibited a stronger binding affinity for HPTS through  $\pi$ - $\pi$  and electrostatic interactions. However, the utility of the host-guest complexes (**1**·HPTS and **2**·HPTS) as an on-off-on fluorescent sensor is limited due to the very high binding constants between **1** and **2** and HPTS.<sup>22</sup>

To further explore the host-guest recognition of **1** and **2** in aqueous media, we decided to investigate the recognition ability of **1** and **2** for amino acids and nucleotides (*e.g.* ATP, ADP, and AMP). Initially, the recognition between **1** and **2** and amino acids was screened by <sup>1</sup>H NMR in D<sub>2</sub>O with phosphate buffer (Fig. S30–S75, ESI<sup>†</sup>). Interestingly, **1** exhibited highly-selective recognition toward tryptophan (Trp), compared to other amino acids (Fig. 3 and Fig. S30, ESI<sup>†</sup>). NMR spectra of the 1:1 mixture of **1** and Trp showed that all proton resonances (H<sub>1'</sub>–H<sub>7'</sub>) of Trp underwent upfield shifts ( $\Delta\delta = 0.14$ – $0.79$  ppm), indicating that the Trp molecule is fully encapsulated into the cavity of **1**. At the same time, the partial protons (H<sub>4'</sub>–H<sub>6'</sub>) of **1** displayed upfield shifts ( $\Delta\delta = 0.04$ – $0.33$  ppm), which could be caused by  $\pi$ -electron shielding of the face-to-face oriented aromatic rings between the  $\pi$ -electron-rich indole moiety of Trp and the  $\pi$ -electron-deficient bipyridinium unit of **1**.<sup>15</sup> Remarkably, compared with that of the protons near the *p*-xylylene ring, the chemical shift of the proton (H<sub>4'</sub>–H<sub>6'</sub>) near the TPE unit in **1** was larger, which indicated that the Trp molecule was closer to the TPE unit in the cavity of **1**. The Job's plot obtained by <sup>1</sup>H NMR in D<sub>2</sub>O (phosphate buffer, pH = 7.4) revealed a 1:1 stoichiometry for the host-guest complex **1**·Trp with a moderate binding constant ( $K_{1\cdot\text{Trp}} = 2.67 \times 10^3 \text{ M}^{-1}$ ) in solution (Fig. S29–S34, ESI<sup>†</sup>). In addition, the binding constant ( $K_{1\cdot\text{Trp}} = 1.21 \times 10^3 \text{ M}^{-1}$ ) and 1:1 stoichiometry of **1**·Trp were also confirmed by ITC experiments (Fig. 3b and Table S2, ESI<sup>†</sup>). Furthermore, ESI-MS also revealed two- and three-charged peaks ([**1**·Trp]<sup>3+</sup> and [**1**·Trp]<sup>2+</sup>), which confirmed the formation of the 1:1 host-guest complex, respectively (Fig. S35, ESI<sup>†</sup>). Then, the limit of detection of the host **1** for Trp was calculated to be 0.36  $\mu\text{mol}$  by

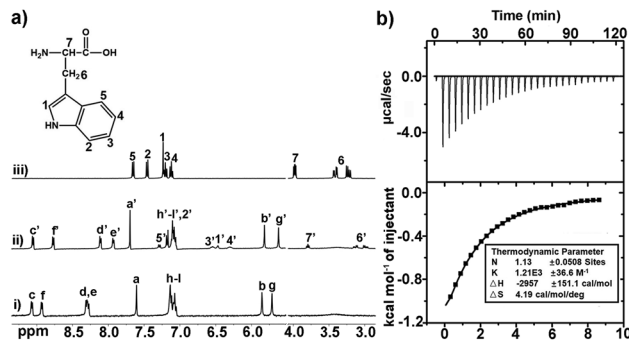


**Fig. 3** (a) <sup>1</sup>H NMR spectra (400 MHz, 298 K, D<sub>2</sub>O, 10 mM phosphate buffer, pH = 7.4) recorded for: (i) **1**·4Cl<sup>-</sup> (0.4 mM); (ii) **1**·4Cl<sup>-</sup> (0.4 mM) and Trp (0.4 mM); (iii) tryptophan (0.4 mM) at 298 K. (b) ITC data for the titration of **1**·4Cl<sup>-</sup> (0.40 mM) in the cell with a solution of Trp (16.0 mM) in the syringe in phosphate buffer (10 mM, pH = 7.4) at 298 K. **1**·4Cl<sup>-</sup>: tryptophan = 1:1. Here, primes (') denote the resonances within the host-guest complexes.

UV-vis experiments (Fig. S36, ESI<sup>†</sup>).<sup>23</sup> Similar but weak recognition behaviours were observed in the case of tyrosine, phenylalanine, aspartic acid, and cysteine with **1**, however, their association constants are too weak to be calculated by NMR or ITC (Fig. S37–S41, ESI<sup>†</sup>). In contrast, **2** showed weaker interactions with all the amino acids on account of its very large cavity (Fig. S56–S75, ESI<sup>†</sup>). For arginine (Asn) and lysine (Leu) as basic amino acids, the  $\alpha$ - and  $\beta$ -protons (H<sub>1'</sub>–H<sub>2'</sub>) of Asn/Leu with **1** and **2** showed downfield shifts, indicating that only electrostatic interactions between the deprotonated carboxyl groups and positive pyridinium groups played a main role (Fig. S42, S43, S62 and S63, ESI<sup>†</sup>).

Next, adenosine derivatives (*e.g.* ATP, ADP, and AMP) as guests were investigated for **1** and **2** as hosts by NMR and ITC. In the <sup>1</sup>H NMR spectrum of **1** with 1.0 equiv. of ATP in D<sub>2</sub>O (phosphate buffer, pH = 7.4), proton resonances (H<sub>1'</sub>–H<sub>2'</sub> and H<sub>6'</sub>–H<sub>7'</sub>) for adenine ( $\Delta\delta_{\text{H}_1'} = 1.50$  ppm and  $\Delta\delta_{\text{H}_2'} = 1.74$  ppm) and ribose moieties ( $\Delta\delta_{\text{H}_2'} = 0.62$  ppm) of ATP were obviously shifted upfield, compared to free ATP, indicating that whole adenine and part of ribose moieties resided in the cavity of **1** (Fig. 4). In addition, the NOESY spectra showed a H<sub>1'</sub>–H<sub>6'</sub> inter-correlation between the adenine moiety of ATP and the TPE unit of **1**, indicating that the adenine moiety of ATP was closer to the TPE unit in the cavity of **1**. The  $\pi$ - $\pi$  interaction between the adenine moiety of ATP and the bipyridinium units of **1** also results in a shielding effect for proton resonances (H<sub>4'</sub>–H<sub>6'</sub>) for the bipyridinium unit in **1**. At the same time, proton resonances for the *p*-xylylene (H<sub>a'</sub>), bridged CH<sub>2</sub> (H<sub>b'</sub>) and neighboring pyridinium (H<sub>c'</sub>) units in **1** were significantly downshifted ( $\Delta\delta = 0.29$  ppm, 0.06 ppm, and 0.18 ppm, respectively), which probably were caused by the electrostatic interactions between the triphosphate unit of ATP and the pyridinium near the *p*-xylylene ring in **1** (Fig. 4). Based on the above NMR data, it was observed that the adenine moiety of the ATP molecule is close to the TPE unit in the cavity of **1**, while the triphosphate unit prefers *p*-xylylene and neighboring pyridinium rings, which is consistent with the result of NOESY spectra (Fig. S77, ESI<sup>†</sup>). On the other hand, the 1:1 host-guest stoichiometry and the binding constant ( $K_a = 1.17 \times 10^4 \text{ M}^{-1}$ ) were determined by ITC (Fig. S78, ESI<sup>†</sup>).

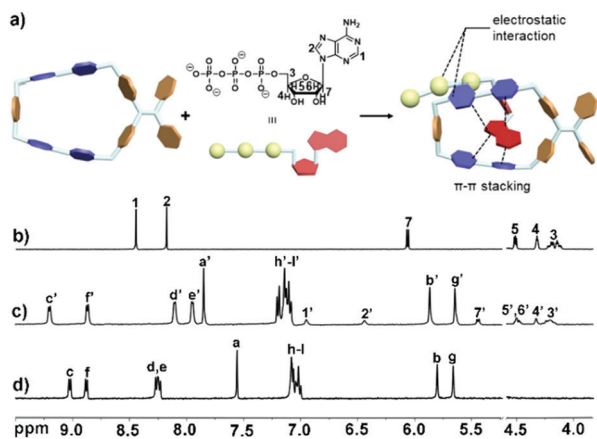


Fig. 4 (a) Schematic representation of 1-ATP;  $^1\text{H}$  NMR spectra (400 MHz, 298 K,  $\text{D}_2\text{O}$ , 10 mM phosphate buffer, pH = 7.4) recorded for: (b) ATP (0.4 mM); (c) 1-4Cl $^-$  (0.4 mM) and ATP (0.4 mM); (d) 1-4Cl $^-$  (0.4 mM). Here, primes (') denote the resonances within the host-guest complexes.

In addition, the limit of detection of the host **1** for ATP was calculated to be 1.89  $\mu\text{mol}$  (Fig. S79, ESI $^\dagger$ ). Similarly, ADP and AMP were quantitatively accommodated within cyclophane **1** to give 1:1 host-guest complexes by  $^1\text{H}$  NMR and ITC. ADP and AMP were bound by **1** with moderate binding constants of  $5.07 \times 10^3 \text{ M}^{-1}$  and  $1.09 \times 10^3 \text{ M}^{-1}$ , respectively (Fig. S80–S83, ESI $^\dagger$ ). Comparing the host-guest interactions of three nucleotides with **1**, their binding ability gradually strengthens, accompanied with the increase of the number of phosphates (Table S2, ESI $^\dagger$ ). All ESI-MS spectra of 1-ATP, 1-ADP and 1-AMP showed the formation of 1:1 host-guest complexes, respectively (Fig. S84–S86, ESI $^\dagger$ ). The results indicated that cyclophane **1** can selectively recognize the ATP molecule through both electrostatic and  $\pi$ - $\pi$  interactions. However, the weak binding behavior between **2** and adenosine derivatives was confirmed by  $^1\text{H}$  NMR and UV-vis studies (Fig. S87–S92, ESI $^\dagger$ ), probably because the large cavity of **2** does not fit with the adenine ring.

In conclusion, we have designed and synthesized two new cationic cyclophanes (**1** and **2**) containing tetraphenylethene and bipyridinium moieties. As determined from their X-ray crystal structures, asymmetrical cyclophane **1** possesses a trapezoid-like and smaller cavity whereas symmetrical cyclophane **2** possesses a flat rectangle-like and larger cavity. Their host-guest behaviours have been investigated by  $^1\text{H}$  NMR, UV-vis, fluorescence and ITC experiments. In aqueous media, the two cyclophanes exhibit a fluorescence quenching effect on the fluorescence indicator HPTS when forming 1:1 host-guest complexes through  $\pi$ - $\pi$  and electrostatic interactions with strong affinity ( $10^8$ – $10^9 \text{ M}^{-1}$ ). More interestingly, **1** exhibited highly-selective recognition for tryptophan and ATP ( $\sim 2$  times to ADP,  $\sim 10$  times to AMP) due to the appropriate size of the cavity and good water-solubility. We anticipate that this kind of cationic cyclophane can also be synthesized and modified with other functional linkers, affording the ability to tune the cavity, host-guest and photophysical properties of these cationic macrocycles, which may find utility in applications such as not only biosensors for detecting biological analytes (e.g. DNA

but also supramolecular building blocks for constructing molecular knots in the near future.

This work was supported by the National Natural Science Foundation of China (21771145 and 21472149 to L. C., 21402151 to Y. Z.).

## Conflicts of interest

There are no conflicts to declare.

## Notes and references

- F. Diederich, P. J. Stang and R. R. Tykwinski, *Modern Supramolecular Chemistry: Strategies for Macrocyclic Synthesis*, Wiley-VCH Verlag GmbH & Co. KGaA, Weinheim, 2008.
- G. W. Gokel, W. M. Leevy and M. E. Weber, *Chem. Rev.*, 2004, **104**, 2723–2750.
- G. Chen and M. Jiang, *Chem. Soc. Rev.*, 2011, **40**, 2254–2266.
- D.-S. Guo and Y. Liu, *Chem. Soc. Rev.*, 2012, **41**, 5907–5921.
- J. Lagona, P. Mukhopadhyay, S. Chakrabarti and L. Isaacs, *Angew. Chem., Int. Ed.*, 2005, **44**, 4844–4870.
- Z. Liu, S. K. M. Nalluri and J. F. Stoddart, *Chem. Soc. Rev.*, 2017, **46**, 2459–2478.
- M. Xue, Y. Yang, X. Chi, Z. Zhang and F. Huang, *Acc. Chem. Res.*, 2012, **45**, 1294–1308.
- (a) M. T. Nguyen, M. D. Krzyaniak, M. Owczarek, D. P. Ferris, M. R. Wasielewski and J. F. Stoddart, *Angew. Chem., Int. Ed.*, 2017, **56**, 5795–5800; (b) W. W. Porter, T. P. Vaid and A. L. Rheingold, *J. Am. Chem. Soc.*, 2005, **127**, 16559–16566.
- C. Cheng, P. R. McGonigal, S. T. Schneebeli, H. Li, N. A. Vermeulen, C. Ke and J. F. Stoddart, *Nat. Nanotechnol.*, 2015, **10**, 547–553.
- (a) E. J. Dale, N. A. Vermeulen, M. Juriček, J. C. Barnes, R. M. Young, M. R. Wasielewski and J. F. Stoddart, *Acc. Chem. Res.*, 2016, **49**, 262–273; (b) H. Y. Gong, B. M. Rambo, E. Karnas, V. M. Lynch and J. L. Sessler, *Nat. Chem.*, 2010, **2**, 406–409; (c) H. Y. Gong, B. M. Rambo, E. Karnas, V. M. Lynch, K. M. Keller and J. L. Sessler, *J. Am. Chem. Soc.*, 2011, **133**, 1526–1533.
- J. Sun, Z. Liu, W. G. Liu, Y. Wu, Y. Wang, J. C. Barnes, K. R. Hermann, W. A. Goddard III, M. R. Wasielewski and J. F. Stoddart, *J. Am. Chem. Soc.*, 2017, **139**, 12704–12709.
- A. Trabolsi, A. C. Fahrenbach, S. K. Dey, A. I. Share, D. C. Friedman, S. Basu, T. B. Gasa, N. M. Khashab, S. Saha, I. Aprahamian, H. A. Khatib, A. H. Flood and J. F. Stoddart, *Chem. Commun.*, 2010, **46**, 871–873.
- J. C. Barnes, E. J. Dale, A. Prokofjevs, A. Narayanan, I. C. Gibbs-Hall, M. Juriček, C. L. Stern, A. A. Sarjeant, Y. Y. Botros, S. I. Stupp and J. F. Stoddart, *J. Am. Chem. Soc.*, 2015, **137**, 2392–2399.
- C. Cheng, P. R. McGonigal, S. T. Schneebeli, H. Li, N. A. Vermeulen, C. Ke and J. F. Stoddart, *Nat. Nanotechnol.*, 2015, **10**, 547–553.
- Q. Chen, J. Sun, P. Li, I. Hod, P. Z. Moghadam, Z. S. Kean, R. Q. Snurr, J. T. Hupp, O. K. Farha and J. F. Stoddart, *J. Am. Chem. Soc.*, 2016, **138**, 14242–14245.
- J. Mei, N. L. C. Leung, R. T. K. Kwok, J. W. Y. Lam and B. Z. Tang, *Chem. Rev.*, 2015, **115**, 11718–11940.
- (a) J. B. Xiong, H. T. Feng, J. P. Sun, W. Z. Xie, D. Yang, M. H. Liu and Y. S. Zheng, *J. Am. Chem. Soc.*, 2016, **138**, 11469–11472; (b) S. Song and Y. S. Zheng, *Org. Lett.*, 2013, **15**, 820–823; (c) C. Zhang, Z. Wang, L. X. Tan, T. L. Zhai, S. Wang, B. Tan, Y. S. Zheng, X. L. Yang and H. B. Xu, *Angew. Chem., Int. Ed.*, 2015, **54**, 9244–9248.
- X. Yan, H. Wang, C. E. Hauke, T. R. Cook, M. Wang, M. L. Saha, Z. Zhou, M. Zhang, X. Li, F. Huang and P. J. Stang, *J. Am. Chem. Soc.*, 2015, **137**, 15276–15286.
- X. Yan, T. R. Cook, P. Wang, F. Huang and P. J. Stang, *Nat. Chem.*, 2015, **7**, 342–348.
- O. Persch, O. Dumele and F. Diederich, *Angew. Chem., Int. Ed.*, 2015, **54**, 3290–3327.
- A. L. Spek, *Acta Crystallogr., Sect. C: Struct. Chem.*, 2015, **71**, 9–18.
- P. P. Neelakandan, M. Hariharan and D. Ramaiah, *J. Am. Chem. Soc.*, 2006, **128**, 11334–11335.
- Q. Lin, Y.-Q. Fan, P.-P. Mao, L. Liu, J. Liu, Y.-M. Zhang, H. Yao and T.-B. Wei, *Chem. – Eur. J.*, 2018, **24**, 777–783.